

Numerical Modeling Study for Fish Screen at River Intake Channel

Jungseok Ho¹, Leslie Hanna², Brent Mefford³, and Julie Coonrod⁴

¹Department of Civil Engineering, University of New Mexico, Albuquerque, NM 87131; PH (505) 573-5079; FAX (505) 277-1988; email: jayho@unm.edu

²Water Resources Research Laboratory, U.S. Bureau of Reclamation, Denver, CO 80225; PH (303) 445-2146; FAX (303) 445-6324; email: lhanna@do.usbr.gov

³Water Resources Research Laboratory, U.S. Bureau of Reclamation, Denver, CO 80225; PH (303) 445-2149; FAX (303) 445-6324; email: bmefford@do.usbr.gov

⁴Department of Civil Engineering, University of New Mexico, Albuquerque, NM 87131; PH (505) 227-3233; FAX (303) 277-1988; email: jcoonrod@unm.edu

Abstract

A numerical modeling study of hydraulic performances of an angled vertical fish screen at a river diversion intake channel that was developed using a porous media numerical scheme. Flow patterns in the intake channel induced by the fish screen were computed with a three-dimensional fluid dynamics computation program solving the Reynolds-averaged Navier-Stokes equations. Screen flow head loss coefficient were simulated and compared with the physical model values converted from the test measurements for the porous media numerical scheme applicability test. For validation of the numerical model, fish screen velocity ratio profiles of sweeping and approach were compared with physical model measurements. Different types of screen face material and baffle installations for uniform approach flow distributions were simulated. The numerical model shows very good agreement with the velocity ratio measurements, and modeling capability for different screen material types and baffle installations by controlling of the numerical model of the porous opening directions and adjustment of baffle porosities respectively.

Introduction

This paper describes numerical model study of hydraulic performances of an angled vertical fish screen at a river diversion intake channel. Porous media numerical scheme was used to model a fish screen, and its application at an intake channel of a rectangular section flume was simulated with a three-dimensional computational fluid dynamics (CFD) code. Flow patterns and transitions around the

screen of the intake channel were provided in this study. Porosity value can be adjusted between zero and one for solid obstacle and porous media respectively, and the flow direction through the screen can be simulated using the porosity opening direction control. The numerical models were calibrated and validated with the physical model measurements completed at the Water Resources Research Laboratory (WRRL) of the U.S. Bureau of Reclamation (USBR) in Denver, Colorado.

For fixed plate screens, the USBR commonly designs for a sweeping velocity at least 10 times an approach velocity for effective cleaning of screens. Two velocity ratios of sweeping to approach 20:1 and 10:1 have been tested under high and low flow rate conditions. Two widely used different face material screens, perforated plate and wedged wire, have been set in the model. Both screens have a porosity of 0.46, but different openings, so that they yield distinctive flow patterns. To test the baffle effects of the uniform flow distribution along the fish screen, adjustable porous baffles, which have been found to have a 20 percent improvement from work of Hanna and Mefford (1999), have been installed behind the screen. In this study, sweeping and approach velocity along the screen was measured and compared with the computed values. In addition, the computations of the screen flow head loss coefficient were compared with the physical model values converted from measurements to test the porous media scheme applicability for the screen material.

The screen model was built series of uniform bays, which is composed of screens, piers, and baffles. These are set up at angles against the inflow direction in the experimental rectangular flume as shown in figure 1. The 20:1 velocity ratio (V_R) and the 10:1 V_R model were angled 2.5 degree and 5.0 degree, respectively, to generate the corresponding ratio sweeping and approach velocity. The dimensions of the model including effective screen length, number of bays, and installation angle are varied depending on the velocity ratio of sweeping to approach. It is assumed that fish move downstream along the screen and enter the bypass channel due to the greater sweeping velocity at the front of the fish screen, while most of water flows into the intake channel through the screen.

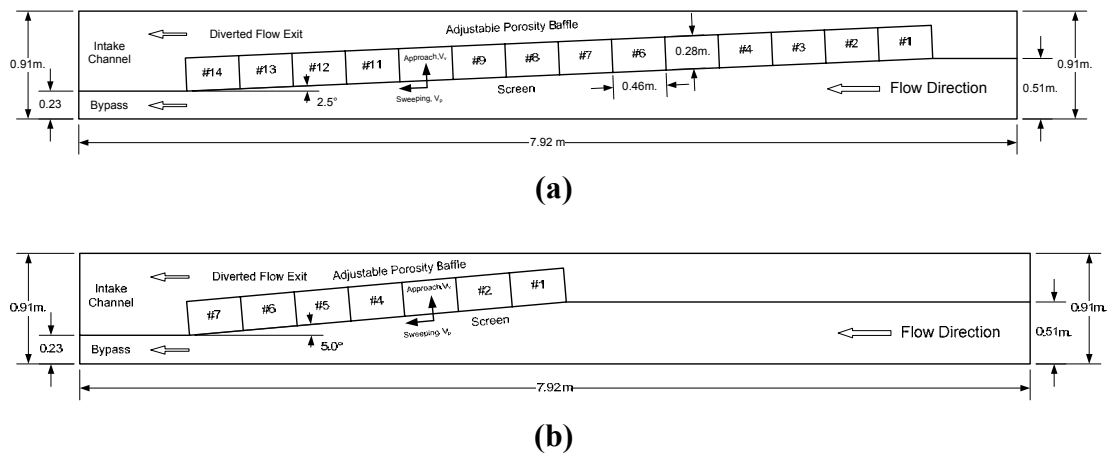


Figure 1. Plane view of fish screen at intake channel model set up with sweeping: approach velocity ratio of: (a) 20:1 V_R model; (b) 10:1 V_R model

Numerical Model

Commercially available CFD code Flow-3D developed by Flow Sciences was used for the numerical modeling in this study. This computer program solves the Reynolds-Averaged Navier-Stokes (RANS) equations by the finite volume formulation obtained from a staggered finite difference grid. For each cell, average values for the flow parameters, pressure and velocity, are computed at discrete times using the staggered grid technique. To solve the RANS equations, the new velocity in each cell is estimated from the coupled momentum and continuity equation as shown below using the initial conditions or previous time step values.

For tracking of the fluid interfaces, the Volume Of Fluid (VOF) method is used. With the VOF method, grid cells are defined as empty, full, or partially filled with fluid. Cells are assigned the fluid fraction varying from zero to one depending on quantity of fluid. Along the fraction cells, advection of fluid handling and the given boundary conditions at the free surface (zero fraction cells) maintain the sharp interface. The free surface slope of a partially filled cell is computed by free surface angle and location of the surrounding cells, and then it is defined by a series of connected chords in 2-D model or by connected planes in 3-D model. These fractions are embedded into all terms of the RANS equations.

Porous Obstacle Generation

In order to define mesh geometry on the finite control volume, the Fractional Area/Volume Obstacle Representation (FAVOR) method, developed by Hirt and Sicilian (1985) is used. The FAVOR method is a porosity technique, which defines an obstacle in a cell with a porosity value between zero and one as the obstacle fills in the cell. Each obstacle within a grid is defined as a volume fraction, (V_F or porosity) to represent a solid condition. To specify regions of variable porosity, the Cartesian direction (x , y , and z) porosities and porous media head loss coefficients K are used in the obstacle generator. The head loss coefficient is applied separately for saturated flow and unsaturated flow conditions. In this model, the local Reynolds number dependent function of the Kozeny-Carman relation (from Jacob Bear, 1988) was used. It is based on the average particle or fiber diameter d , and linear and quadratic head loss equations can be combined into a single expression for the head loss coefficient:

$$K = \frac{\mu}{\rho} \frac{1-V_F}{V_F^2} \left[\frac{\alpha}{d^2} (1-V_F) + \frac{\beta}{d^2} Re \cdot V_F \right]$$

where μ and ρ are the viscosity and the density of the fluid respectively; α is a constant with a typical value of 180 and β is a roughness factor which ranges between 1.8 and 4.0; d is the average fiber diameter. Volume fraction, V_F is the porosity of the medium, and the Reynolds number $Re = \rho u d / \mu$ (Flow Science, 2003). The head loss coefficient K is converted in this code into the dimensionless quantity $K_{DRG} = 1/(1+K\Delta t)$, where Δt is the time step size, and added to the governing momentum equations.

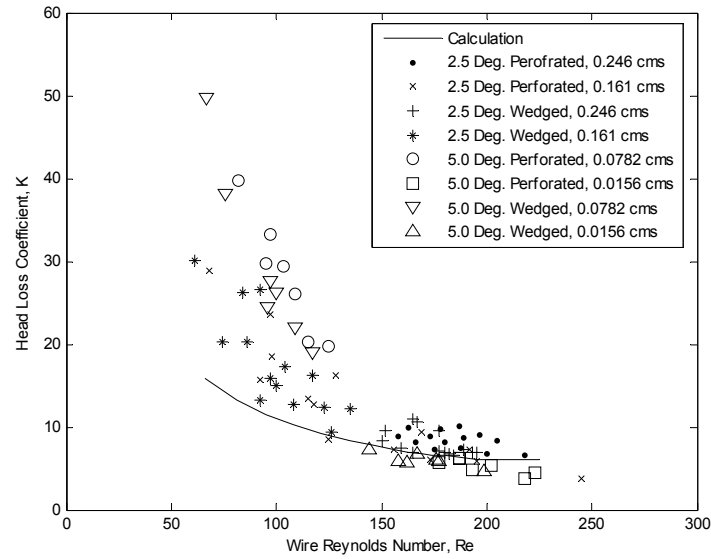


Figure 2. Head loss coefficient versus wire Reynolds number relationship for angled vertical screens

Numerical Model Implementation

Solid obstacle of the guiding walls and porous media of the screen and baffles are meshed on approximately 7.9 m long by 9.2 m wide by 4.5 m high of the three-dimensional grid domain. To save computational time and memory, various sizes of the hexagon grid cells were meshed ranging from 14.3 cm³ to 162 cm³ in volume. This grid was modified to a finer grid after the initial computation to reach steady state condition. The perforated plate model was defined by a perpendicular direction opening (y -direction porosity) of the porous media. For modeling of the wedged wire, both perpendicular and horizontal opening directions (y - and x -direction porosity) were combined to the screen porosity. These screen models have the same porosity of 0.46 and zero vertical (z -direction) openings. For the upstream and downstream boundary condition, the stagnation pressure value was specified. The stagnation pressure, $P + \rho V^2/2$, boundary condition assumes that the fluid next to the boundary is stagnant at the specified pressure value which is an approximation to a large reservoir of fluid outside the mesh domain (Flow Science, 2003). In this model, fluid heights of 47.2 cm and 38.5 cm for the 20:1 V_R model and 34.6 cm and 30.3 cm for the 10:1 V_R model were used for the stagnation pressure boundary conditions. However, the continuative boundary condition, which consists of zero normal derivatives at the boundary for a smooth continuation of the flow through the boundary, was adapted for the downstream boundary condition to evaluate the outflow rate at the downstream with the physical test measurement. Atmospheric pressure was set at the top of the mesh, and no slip wall condition, which is defined as having zero tangential and normal velocities, was applied at bottom and sidewall of the mesh.

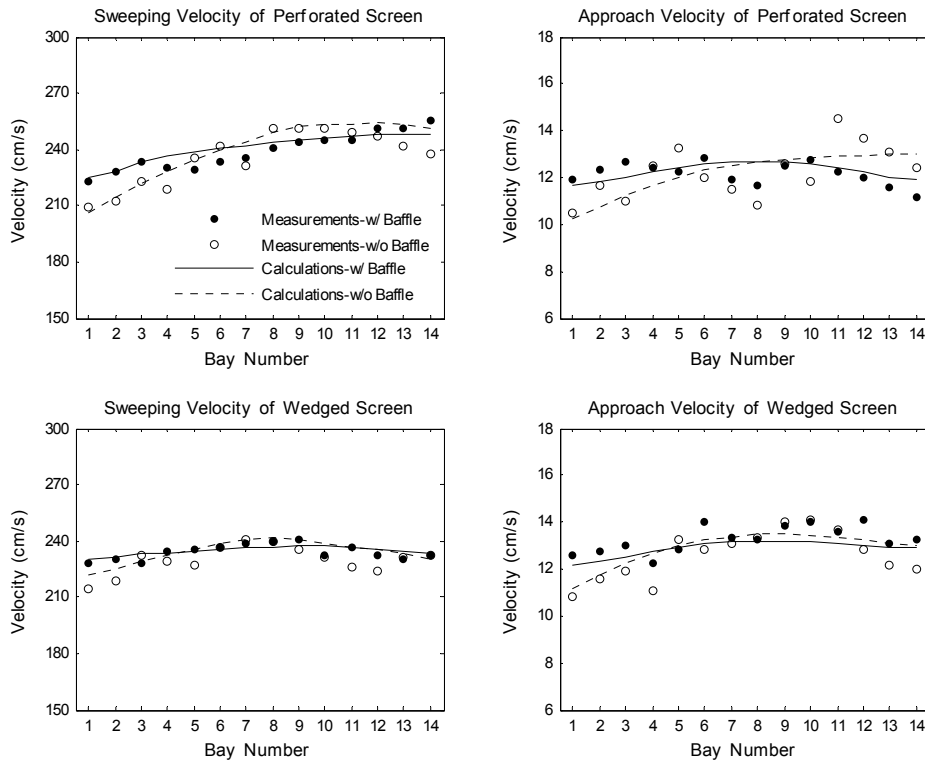


Figure 3. Velocity comparison of 20:1 V_R model at $2.46e5 \text{ cm}^3/\text{s}$ flow rate

Physical Model

For the 20:1 V_R model test, 6.1 m of effective length of vertical screen are set an angle of 2.5 degree against flow direction in a 0.91 m wide by 0.61 m deep rectangular flume. The screen is divided into 14 bays that are made of 3.8 cm wide plywood piers spaced 46 cm apart. The 10:1 V_R model has 7 bays with 3.05 m effective length of vertical screen installed at an angle of 5.0 degree. Perforated plate with 2.38 mm diameter openings in 46% open area screen was modeled. Once these tests were completed, wedged wire with 1.75 mm wire width and 1.5mm slot openings was installed in the model. Perforated baffles positioned 28 cm behind the baffles were adjusted in each bay to provide a uniform approach flow distribution along the full length of the screen. Depth-averaged sweeping and approach velocities were measured using a three-component acoustic doppler-velocimeter probe at a distance of 7.6 cm from the screen face at the center of each bay. The tests were executed under two design considerations: the different types of screen face material applications and the porous baffle effects. These scenarios were applied in both the 20:1 V_R and the 10:1 V_R models over four flow rate conditions: $1.61e5 \text{ cm}^3/\text{s}$ and $2.46e5 \text{ cm}^3/\text{s}$ for the 20:1 V_R model, and $1.56e4 \text{ cm}^3/\text{s}$ and $7.82e4 \text{ cm}^3/\text{s}$ for the 10:1 V_R model.

Modeling Results

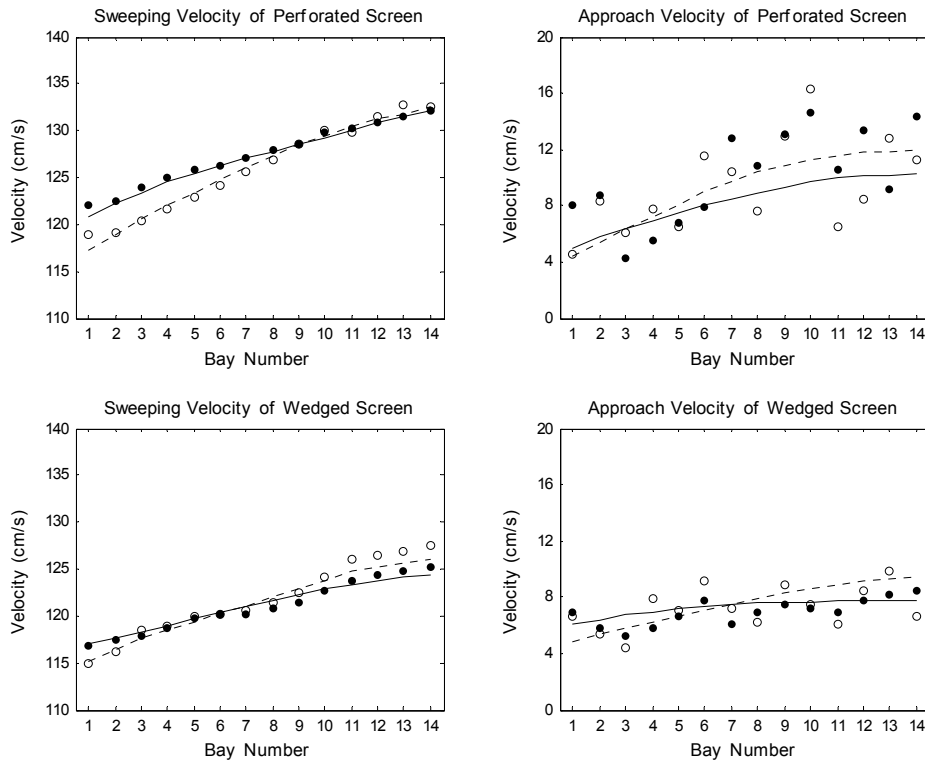


Figure 4. Velocity comparison of 20:1 V_R model at $1.61e5 \text{ cm}^3/\text{s}$ flow rate

The screen flow head loss coefficient of each bay and the velocity ratio along the screen were measured to validate the fish screen intake channel numerical model. Figure 2 illustrates the measured values of the head loss coefficient with the wire Reynolds number of the screen with angle orientation of 2.5° for the 20:1 V_R model and 5° for the 10:1 V_R model to the flow. The non-baffled screen model approach velocity and head loss of each bay were adopted in the energy equation, $\Delta h = KV^2/2g$, over the wire Reynolds number, $R_w = Vw/v$, where w is an opening of the screen wire space and v is the kinematic viscosity of the fluid. A maximum head loss of 0.55 cm was observed in both the perforated plate and the wedged wire screen. No significant difference of the flow approach angle and screen face material effect was observed in head loss coefficient values ranging from 3.7 to 49.8. The 10:1 V_R model at the higher flow rate ($7.82e4 \text{ cm}^3/\text{s}$) condition models have a steeper slope, while the 20:1 V_R model perforated plate screen model, which is plotted by hollow circle shows wider range of the head loss coefficient over the wire Reynolds number. The solid line indicates calculated values of the head loss coefficient. It is converted from the dimensionless drag from the computations of the head loss coefficient values by the formula as discussed in the previous section. This numerical calculation shows very good estimation for the wire Reynolds number higher than 140, and is becoming steady at values higher than 200. For $R_w < 140$, the numerical model is not sensitive enough to the wire Reynolds number, but still shows the inverse relationship of the measurements.

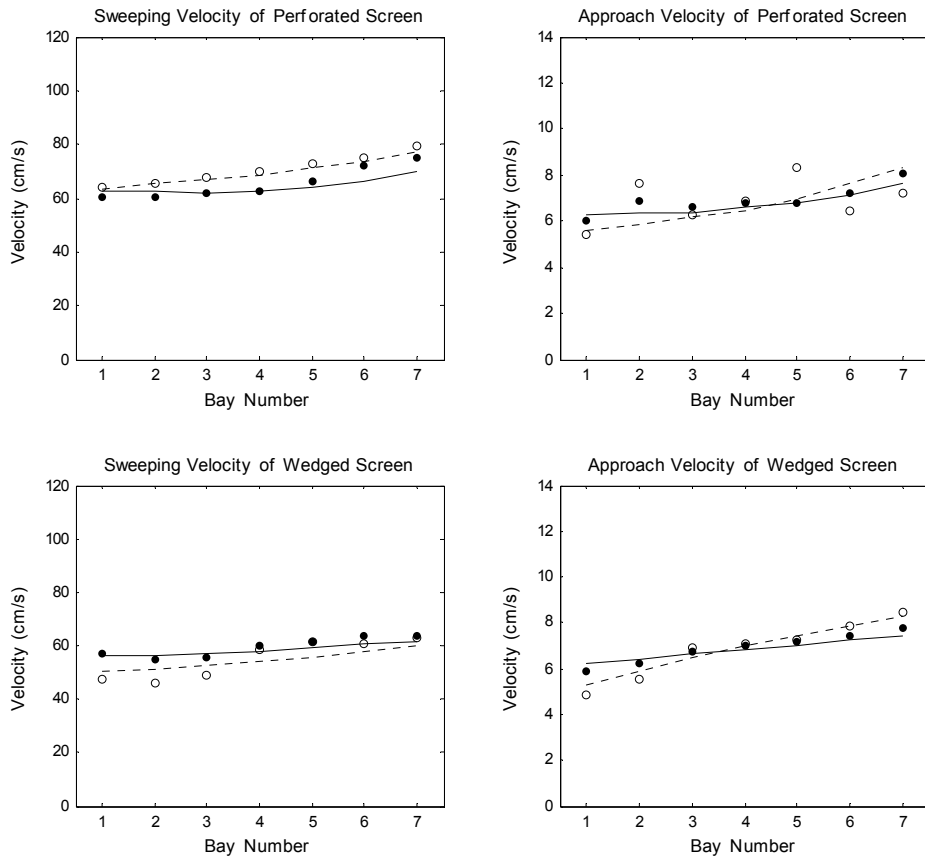


Figure 5. Velocity comparison of 10:1 V_R model at $7.82 \times 10^4 \text{ cm}^3/\text{s}$ flow rate

Computed values of the parallel and adjacent component of velocity and the perpendicular component velocity were compared with the physical model measurements. The computed x and y -components of velocity at each bay were transformed to the parallel and perpendicular velocities considering the screen angle orientation. Figure 3, 4, 5, and 6 shows a series of profiles for the sweeping velocities and approach velocities of the 20:1 V_R and the 10:1 V_R models. Two sets of velocity profiles along the bays show the baffle effects for uniform velocity distributions in each flow condition test. Bay #1 indicates the upstream end at the channel entrance, and bay #7 and #14 are at the downstream end next to the bypass channel in figure 1. Solid circles and hollow circles represent the physical model measurements of the with-baffle model and non-baffle model respectively. To compare the measurements, numerical model computations under identity conditions are plotted with solid and dotted lines.

For the 20:1 V_R model, passing $2.46 \times 10^5 \text{ cm}^3/\text{sec}$ flow rate of water in the flume, the physical model sweeping velocity varied between 209 cm/s and 265 cm/s when the approach velocity was between 10.0 cm/s and 15.5 cm/s. Average flow depth along the screen was approximately 20.3 cm. In the case of $1.61 \times 10^5 \text{ cm}^3/\text{sec}$ of flow passing in an average of 27.6 cm water depth, sweeping and approach velocities varied from 115 cm/s to 128 cm/s and 4.0 cm/s to 16.0 cm/s respectively.

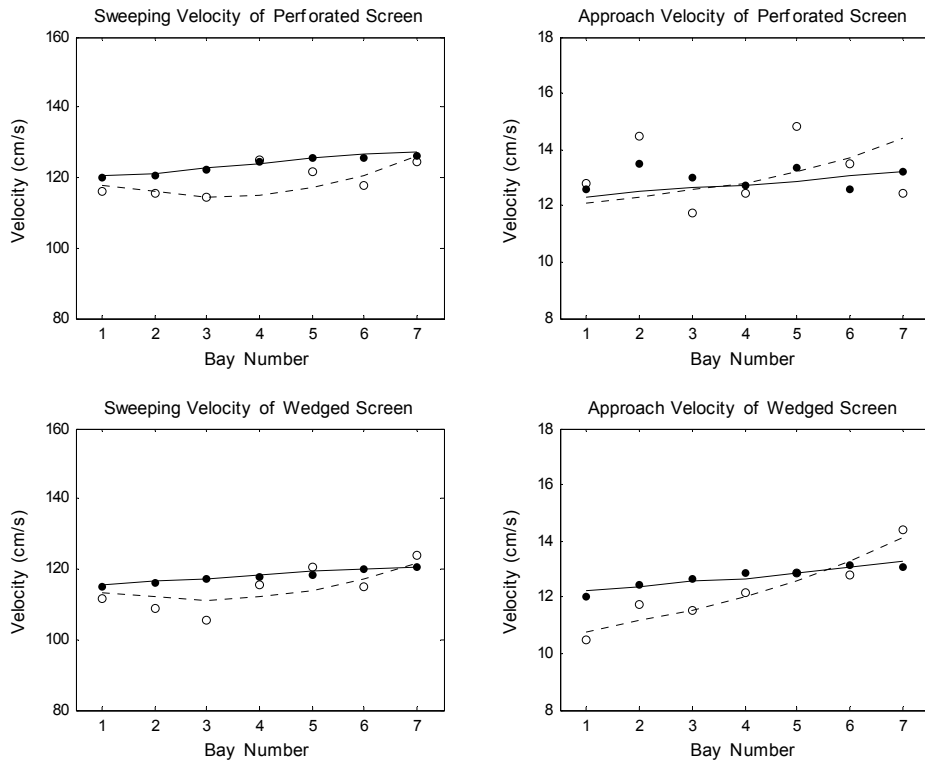


Figure 6. Velocity comparison of 10:1 V_R model at $1.56e4 \text{ cm}^3/\text{s}$ flow rate

In the perforated plate screen test, the velocity ratio of sweeping and approach varied from 0.051 to 0.078 compared to the design ratio of 0.05 of the 20:1 V_R model. As seen in figure 4, the approach velocity of the $1.61e5 \text{ cm}^3/\text{sec}$ case varies widely and increases downstream to the bypass exit channel. On the other hand, the wedged wire screen test shows relatively little velocity ratio change of 0.056 and 0.057. The baffled screen model, shown by solid circle profiles, show more uniform flow distribution along the screen than the non-baffled screen model, shown by hollow circle profiles, for most cases as shown in figure 3 and 4. The baffled model velocity profile slopes are lower and flatter than the non-baffled model for both sweeping and approach velocity profiles. The solid and dotted lines represent the numerical model computations of the baffled and non-baffled model respectively. As shown, the numerical model computations are in good agreement with the physical model measurements.

The 10:1 V_R model was completed for two flow rate conditions. In the case of $7.82e4 \text{ cm}^3/\text{sec}$ flow rate of water passing in the approximately 26.9 cm average water depth in the flume, sweeping and approach velocities varied from 59.8 cm/s to 79.5 cm/s and 5.4 cm/s to 8.1 cm/s respectively. When the flume flow rate was $1.56e4 \text{ cm}^3/\text{sec}$ and 26.7 cm water depth flow conditions, the velocity ranged from 116 cm/s to 126 cm/s for the sweeping component and from 11.3 cm/s to 14.9 cm/s for the approach component. Using the perforated plate screen, the velocity ratio of sweeping and approach were 0.110 and 0.105 in comparison to the 0.1 design velocity ratio. These results are more accurate than the 20:1 V_R model test

measurements, and both sweeping and approach velocity profiles are more stable and linear than the 20:1 V_R model test results as shown in figure 5. In the wedged wire screen test, the velocity ratios were slightly higher than the perforated plate screen as 0.108 and 0.106 in comparison to the 0.1 fraction of the design velocity ratio. The baffle is more effective in providing uniform flow distributions along the screen in the 10:1 V_R model also. As seen in figure 6, the baffled model velocity profile slope is lower and flatter than the non-baffled model for both sweeping and approach velocity profiles. Very good agreement was found between the numerical model computations and physical model measurements.

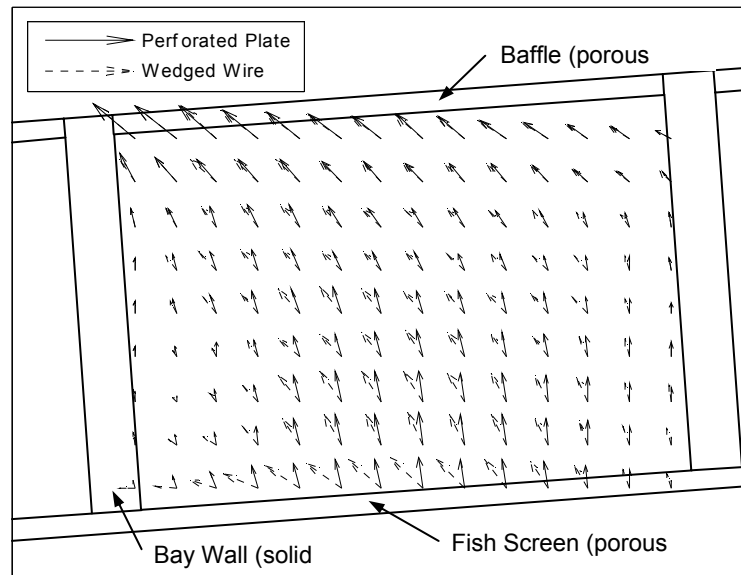


Figure 7. Velocity vector comparison between perforated plate and wedged wire screen

Figure 7 shows comparison of two-dimensional velocity vector computations between the perforated plate screen model and the wedged wire screen model at bay #4 of the 10:1 V_R model under a $7.82e4 \text{ cm}^3/\text{s}$ flow rate. The solid and dotted arrows represent the velocity vectors through each the wedged wire screen and the perforated plate screen tests respectively. As seen, the velocity vectors of the wedged wire screen application test are passing the screen toward the left side of the bay, while the velocity vectors of the perforated plate screen application test are passing the screen vertically.

Conclusion

The porous media scheme can be used to numerically model a fish screen and its application in the river intake model. Screen flow head loss coefficients were simulated and compared well with the physical model values converted from the test measurements for the porous media numerical scheme applicability test. The computations of the velocity ratio of sweeping to approach, which was employed for

numerical model validations, show very good agreement with the physical model measurements. In addition, it is shown that the different screen face materials application and the baffle application for uniform flow distribution can be simulated with good accuracy by control of the porous opening direction of the screen and adjustment of baffle porosity respectively. The porous media numerical scheme can be a simple and effective substitution for numerical modeling of various types of fish screen facilities.

Acknowledgements

The writers wish to thank James Higgs and Billy Baca for many valuable suggestions of the numerical model and physical model test data collections at the Water Resources Research Laboratory of the U.S. Bureau of Reclamation, Denver, Colorado.

References

- Flow-3D user manual; excellence in flow modeling software, v 8.2. (2003). Flow Science, Inc., Santa Fe, NM.
- Hanna, L. J., and Mefford, B. W. (1999). "Hydraulic Model Studies of Contra Costa Canal Fish Screen Structure and Trash Rake." *R-99-05*, WRRL, USBR, U.S. Department of the Interior Denver, CO.
- Hirt, C. W., and Sicilian, J. K. (1985). "A porosity techniques for the definition of obstacles in rectangular cell meshes." *Proc., 4th Int. Conf. Ship Hydro.*, National Academy of Science, Washington, D.C., 1-19.
- Jacob, Bear (1988). *Dynamics of Fluids in Porous Media*. Dover, New York.